Granular Simulation of NEO Anchoring

Hammad Mazhar[1]

Introduction

NASA is interested in designing a spacecraft capable of visiting a Near Earth Object (NEO), performing experiments, and then returning safely. Certain periods of this mission will require the spacecraft to remain stationary relative to the NEO. Such situations require an anchoring mechanism that is compact, easy to deploy and upon mission completion, easily removed.

The design philosophy used in the project relies on the simulation capability of a multibody dynamics physics engine. On Earth it is difficult to create low gravity conditions and testing in low gravity environments, whether artificial or in space is costly and therefore not feasible. Through simulation, gravity can be controlled with great accuracy, making it ideally suited to analyze the problem at hand.

Using Chrono::Engine [1], a simulation package capable of utilizing massively parallel GPU hardware, several validation experiments will be performed. Once there is sufficient confidence, modeling of the NEO regolith interaction will begin after which the anchor tests will be performed and analyzed. The outcome of this task is a study with an analysis of several different anchor designs, along with a recommendation on which anchor is better suited to the task of anchoring. With the anchors tested against a range of parameters relating to soil, environment and anchor penetration angles/velocities on a NEO.

Simulation Capability

The simulation of multiple rigid bodies at an extreme scale becomes an increasingly parallelizable problem difficult to run on today's sequential processors in a meaningful amount of time. Until recently, the high cost of parallel computing limited the analysis of such large systems to a small number of research groups. This is rapidly changing, owing in large part to general-purpose computing on the GPU (GP-GPU). GP-GPU computing has been very vigorously promoted by NVIDIA since the release of the CUDA development platform [2], an application interface for software development targeted to run all NVIDIA GPUs. A large number of scientific applications have been developed using CUDA, most of them dealing with problems that are quite easily parallelizable such as molecular dynamics or signal processing. Very few GP-GPU projects are concerned though with the dynamics of multibody systems, the two most significant being the Havok [3] and the NVIDIA PhysX [4] engines. Both are commercial and proprietary libraries used in the video-game industry and their algorithmic details are not public. Typically, these physics engines trade precision for efficiency as the priority is in speed rather than accuracy. In this context, the goal of our effort was to somewhat de-emphasize the efficiency attribute and instead implement an open source, general-purpose physics-based GPU solver for multibody dynamics backed by convergence results that guarantee the accuracy of the numerical solution.

---

[1] Visiting summer student from University of Wisconsin-Madison, at JPL under Space Grant Program.

Unlike the so-called penalty or regularization methods, where the frictional interaction can be represented by a collection of stiff springs combined with damping elements that act at the interface of the two bodies, the approach embraced here draws on time-stepping procedures producing weak solutions of the differential variational inequality (DVI) problem, which describes the time evolution of rigid bodies with impact, contact, friction, and bilateral constraints.

Recent approaches based on time-stepping schemes have included both acceleration-force linear complementarity problem (LCP) approaches [5] and velocity-impulse, LCP-based time-stepping methods [6]. The LCPs, obtained as a result of the introduction of inequalities accounting for non-penetration conditions in time-stepping schemes, coupled with a polyhedral approximation of the friction cone, must be solved at each time step in order to determine the system state configuration as well as the Lagrange multipliers representing the reaction forces. If the simulation entails a large number of contacts and rigid bodies, as is the case for granular materials, the computational burden of classical LCP solvers can become significant. Indeed, a well-known class of numerical methods for LCPs based on simplex methods, also known as direct or pivoting methods [7], may exhibit exponential worst-case complexity. Moreover, the three-dimensional Coulomb friction case leads to a nonlinear complementarity problem (NCP). The use of a polyhedral approximation to transform the NCP into an LCP introduces unwanted anisotropy in friction cones and significantly augments the size of the numerical problem.

In order to circumvent the limitations imposed by the use of classical LCP solvers and the limited accuracy associated with polyhedral approximations of the friction cone, a parallel fixed-point iteration method with projection on a convex set has been developed [8]. The method is based on a time-stepping formulation that solves at every step a cone-constrained quadratic optimization problem. The time-stepping scheme has been proved to converge in a measure differential inclusion sense to the solution of the original continuous-time DVI. Using this method a GPU based simulation capability was implemented in the open source Physics Engine: Chrono::Engine [1].

Short Range Interaction Forces

In low gravity environments, gravitational forces become less prevalent in comparison to cohesive and electrostatic forces. Table 1 [9], shows that as the gravitational force decreases, the radius at which the attractive forces between particles of lunar regolith become equivalent to gravitational forces increases as gravity decreases. In order to simulate the effects of short range forces, the simulation capability was augmented with support for an additional contact based force system.

Gravity [Gs]	Grain Radius [m]	Analog body
1	$6.5\ x\ 10^{-4}$	Earth
.1	$2\ x\ 10^{-3}$	Moon
.01	$6.5\ x\ 10^{-3}$	Vesta (180 km)
.001	$2\ x\ 10^{-2}$	Eros (10km)
.0001	$6.5\ x\ 10^{-2}$	Toutatis (1.8 km)
.00001	$2\ x\ 10^{-1}$	Itokawa (.18) km
.000001	$6.5\ x\ 10^{-1}$	(.018 km)
.0000001	$2\ x\ 10^{-0}$	KW4 Equator

Table 1 : Assuming Lunar Regolith, This table shows the radius at which weight and cohesion forces become equivalent, along with parent body sizes.

Unlike frictional forces, which act at the surface of an object, interaction forces such as cohesion can apply within a certain boundary around an object. For example, Figure 2 shows the intersection of two boundaries. This interaction distance acts as the cutoff for the force. When there is contact between the two boundaries, a force is applied to both objects, when they separate the force becomes zero.

Short range interaction forces are modeled using a fixed boundary/envelope around each collision geometry. Figure 1 shows envelopes around a sphere and a box. An additional collision detection phase is performed using the envelopes rather than the actual collision geometry. This collision detection phase yields a list of intersections that are then processed in parallel; each contact gets an associated force. It is possible for objects to have multiple forces from multiple envelope intersections. A reduction step is performed to compute the resultant force and apply it to each object.

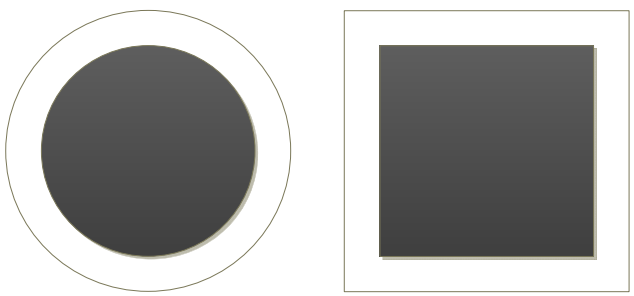

Figure 1: Object Envelopes

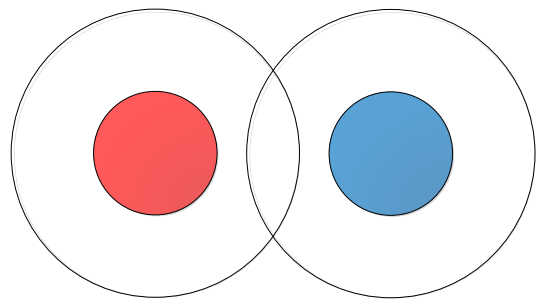

Figure 2: Interaction between objects

For Lunar Regolith, cohesion operates on separation distances of $10^{-10}[m]$, this distance relates to the surface cleanliness of the regolith **[10]**. Surface cleanliness, $S = 1.5 * 10^{-10}/t$, where t is the separation distance, is a measure of how close particles can get to each other. For example on earth, due to water molecules and gases in the atmosphere, the surface cleanliness is close to .1, on the side of the moon facing the sun, however, the surface cleanliness is close to unity. Because the amount of molecules and gases that are deposited on the free surface of the regolith is small, the van der Waals force between regolith particles is large. This force is given by Equation 1 and using parameters from Table 2, can be simplified to the form in Equation 2 [9].

A - Hamaker Coefficient	$4.3x10^{-20}[J]$
S – Surface Cleanliness	$.1 \rightarrow 1$
Ω - Omega	$1.5x10^{-10}\ [m]$
R – Reduced Radius	$\mathrm{R} = \frac{r_1 r_2}{r_1 + r_2}$

Table 2 : Parameters associated with cohesion

$$F_c = \frac{AS^2R}{48\Omega^2}$$

Equation 1: Cohesive force model

Simplifies into:

$$F_c = 3.6x10^{-2}S^2R$$

Equation 2: Simplified cohesive force model

Settling Behavior

In order to capture short range interaction forces properly, it is important that the granular material not interpenetrate. There are several ways to reduce the amount of interpenetration: Reduce time step, increase the number of LCP iterations, and increase the responsiveness of each LCP iteration. To better understand the behavior of the parallel LCP solver a parametric study was performed using these three parameters.

LCP Iterations	100	200	400	600	800	1000
Iteration Scaling factor	0.1	0.2	0.4	0.6	0.8	1.0
Timestep [s]	0.005	0.0025	0.001	0.0005	0.00025	

Table 3 – Parameters for parametric study

Figure 3

The parameters in Table 3 were used to run 180 different simulations consisting of a long slender box in which 10 spheres were dropped. The width of the box was slightly larger than the width of the sphere, keeping the spheres stacked on top of each other, see Figure 3. Each simulation was run for 5 seconds and the kinetic energy was measured for the entire system. If the rate at which the kinetic energy decreases is higher, the system reaches a state of rest faster with less interpenetration. When the energy is low but hasn't reached zero, it means that objects are still moving and slowly sinking into one another. Figure 4 shows the results for a simulation with 100 LCP iterations and a .1 scaling factor. When comparing to Figure 5, which is 1000 iterations with a .1 scaling factor, the rate at which the kinetic energy decreases to zero is much greater. It is possible to converge to a stable configuration faster with less iterations if the LCP scaling factor is higher, see Figure 6, where the scaling factor is .8. However, this causes the solver to become unstable when large penetrations do occur as it corrects for them faster, causing large changes in velocity. When velocities become too large, problems with tunneling (objects passing through one another) can occur, further destabilizing the simulation.

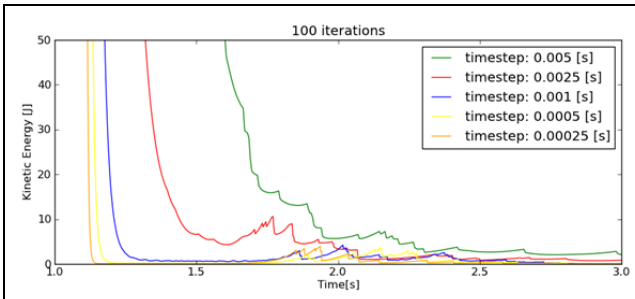

Figure 4 : Simulation with a LCP scaling factor of .1 and 100 LCP iterations

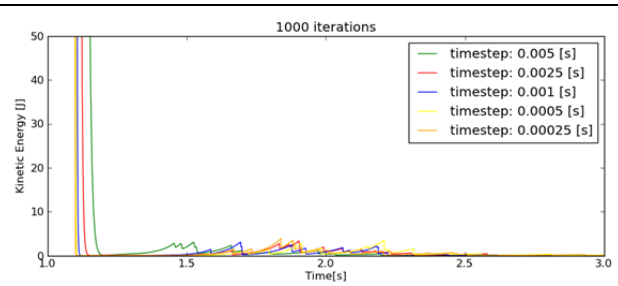

Figure 5: Simulation with a LCP scaling factor of .1 and 1000 LCP iterations

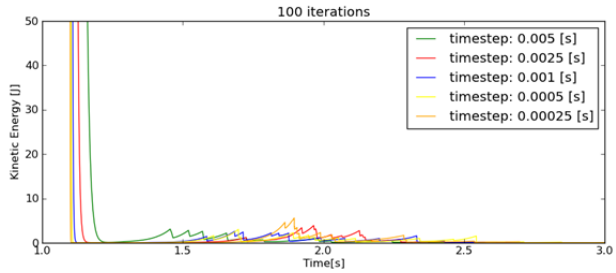

Figure 6: Simulation with a LCP scaling factor of .8 and 100 LCP iterations

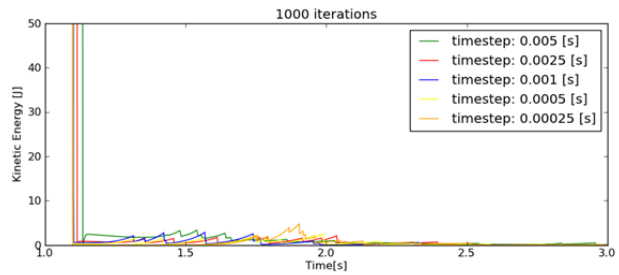

Figure 7: Simulation with a LCP scaling factor of .8 and 1000 LCP iterations

Simulation Results

Brazil Nut Test

A simulation of the Brazil nut experiment [11], was completed based on parameters from [12]. If granular material of two different sizes and densities is placed in the same container and the container is excited with a specific sinusoidal motion, the two materials can be separated with great control. This segregation process is used widely in manufacturing and is a heavily documented phenomenon. A more thorough study will be performed using various granular materials and parameters so that results can be compared to those in literature. Macro level effects have been confirmed; see Figure 8, where the white sphere moves upwards due to the vibration of the container at 30 Hz.

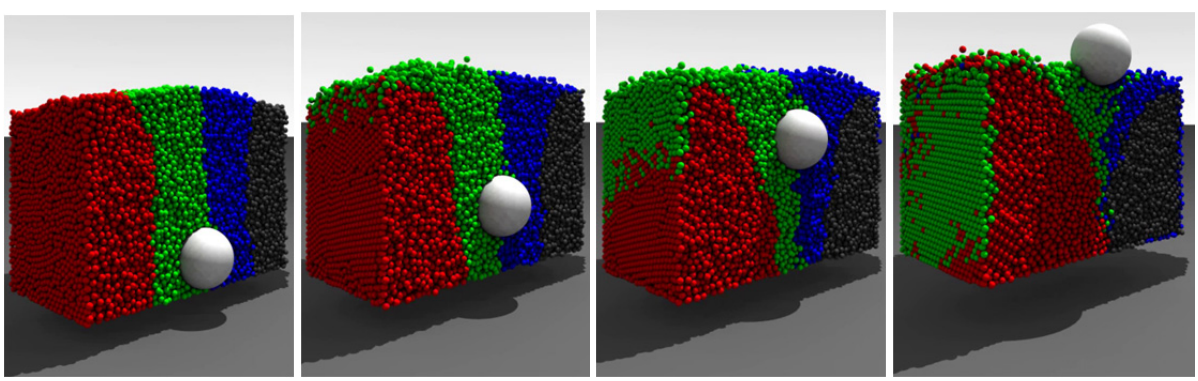

Figure 8: Brazil Nut Simulation – As the container full of granular material is vibrated, the large ball slowly moves upwards.

Ball Drop Experiment

This experiment involves a bed of granular material and a relatively large heavy ball (or impactor) falling into that material. The acceleration profiles of the ball are measured as it is dropped onto the granular material. To simulate the ball drop test, an initial set of test data was created. 250,000 equally sized particles were dropped into a box and allowed to come to a stable state of compaction. This set of data was saved and is reused for each parametric test where the impactor parameters are varied. For tests where the particle parameters are varied, different initial data sets were created. For every combination of impactor and particle type, the position,

acceleration, and velocity profiles of the impactor were saved. These profiles were used to make comparisons against experimental data provided in [13].

Currently, particles with a radius of .0035 meters have been simulated for each impactor. Results showed, when compared to literature, that the acceleration caused by the impact was too great and the depth of impactor penetration was too low. The next step is to determine the cause of the inconsistency. Parameters such as the friction coefficient of the walls or the surface of the impactor could be contributing factors to the differences seen. Table 1 shows the full list of particle and impactor parameters that are being simulated.

Particle			Impactor	
Size [m]	Density[kg/m^3]	Friction ∠	Rad [m]	Mass [kg]
.0035	1560	23	0.095	0.034
.012	720	28	0.013	0.083
.0005	5490	24	0.015	0.13
.0017	5490	24	0.02	0.287
Container:			0.025	0.531
Width	Thickness		0.035	1.437
.6 [m]	.03[m]		0.04	2.099
			0.045	3.055
			0.05	4.079
			0.013	0.064
			0.019	0.201
			0.026	0.518
			0.0125	0.009
			0.019	0.018

Table 4 : Particle, Impactor and Container parameters

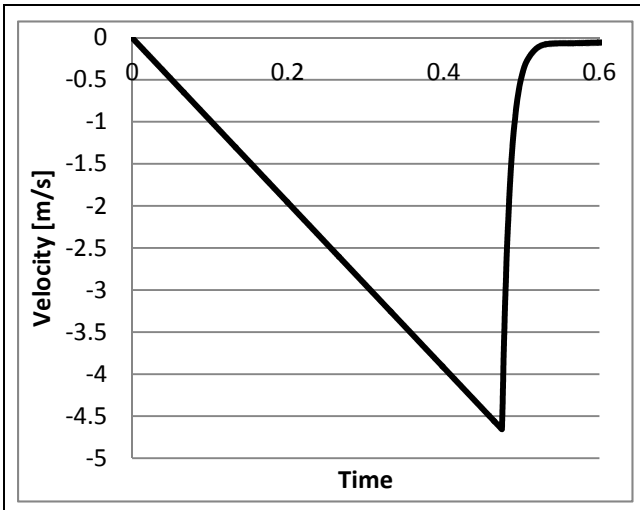

Figure 9: Velocity profile of impactor colliding with the bed of granular material.

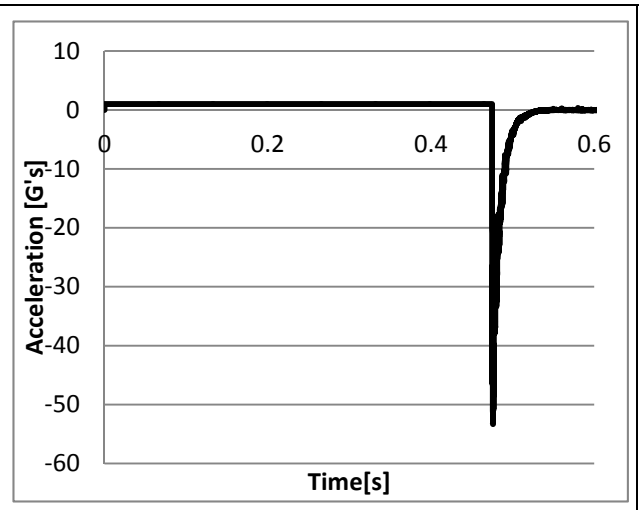

Figure 10: Acceleration profile of impactor colliding with the bed of granular material.

Anchoring Experiments

Using the initial test data created for the parametric ball drop test, helical anchors, such as those in Figure 11, penetrate and anchor into a bed of granular material. Currently, the simulation uses an anchor with a mass of 1 kg which is inserted with a vertical force of 10 N and an axial torque of 10 N-m. Once the anchor penetrates and digs into the material, it is pulled out with a force of 20 N-m. The purpose of this experiment is to set the underlying framework required to test anchors penetrating at different angles, masses, velocities and torques. The force/torque required to remove the anchor from the granular material is measured to determine the effect of different granular materials on the performance of the anchor.

Initially a triangular mesh was to be used for the anchor geometry. This method did not perform well due to the number and size of the triangles in the mesh, which increased the total number of contacts. Therefore, a different approach that involves using geometric primitives was explored. In this approach the anchor is modeled using boxes, cylinders, and spheres. Using primitives rather than a triangulated mesh allows the anchor to be parameterized easily.

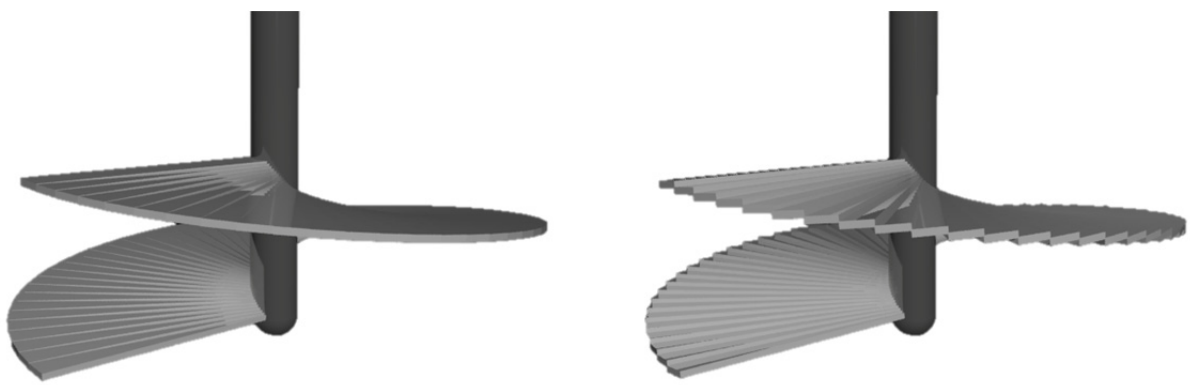

Figure 11: Anchor designed using geometric primitives. Right anchor is created using 67 boxes, 1 cylinder and 1 sphere. If the boxes are rotated along their horizontal axis by 10 degrees, the left anchor is created.

A simulation of a helical anchor, penetrating a bed of granular material can be seen in Figure 12. In this simulation, an initial bed of granular material was simulated until the kinetic energy of the system was almost zero. Once this bed was created an anchor was dropped spinning at a constant rate of π radians per second. After three seconds the anchor was pulled out of the bed at a constant velocity until it was completely free.

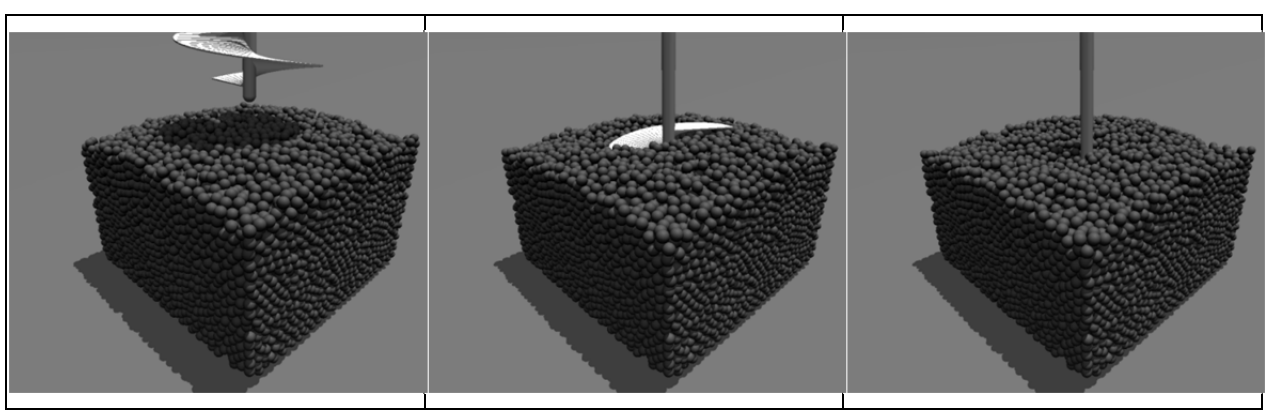

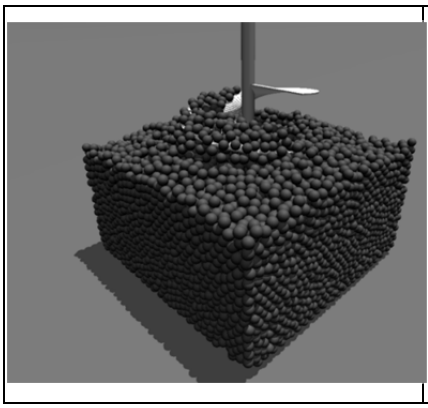	Anchor Mass: .25 $[kg]$ Bead Mass: 2.802 E-04 $[kg]$ Bead Radius: .0035 $[m]$ Bead Density: 1560 $[kg/m^3]$ μ_{bead}: .4245	$h\ (timestep)$: .0005 $[s]$ G: $-9.80665\ \left[\frac{m}{s^2}\right]$ Particles: 20000 Container width: .1 $[m]$ $\mu_{container}$: .5

Figure 12: Helical anchor digging into the bed of particles, under gravity, and then being pulled out at a constant velocity.

Collision Detection

Several tests were run using different collision detection methods on the GPU. This was to make sure that results from one algorithm were in agreement with one another. The following algorithms were tested:

Sphere - Sphere [Specific code]	Ellipsoid - Ellipsoid [Specific code]
Sphere - Sphere [Convex code]	Ellipsoid - Ellipsoid [Convex code]

In this simulation spheres were dropped in a 10x10x10 configuration into an enclosed box Figure 13, and an open plate, Figure 14. For the enclosed box, the expected and observed contact behavior was an initial increase in contacts and then a leveling off as the objects settled. For the plate the contacts initially increased and as particles flowed off the plate a gradual decrease occurred.

Due to the iterative nature of the convex and ellipsoid collision detection algorithms, there are numerical differences in the solutions and therefore the number of contacts detected in a simulation. Progress was made in solving errors and tuning of collision detection parameters. Results are in better agreement than previous tests.

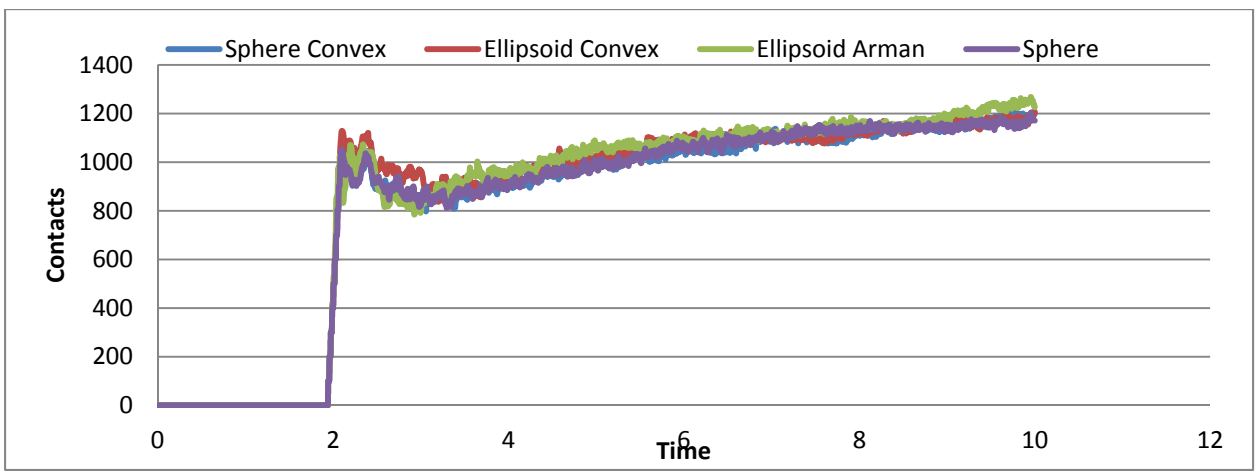

Figure 13: Contact Test 1, a 10x10x10 cube of spheres dropped into an enclose container.

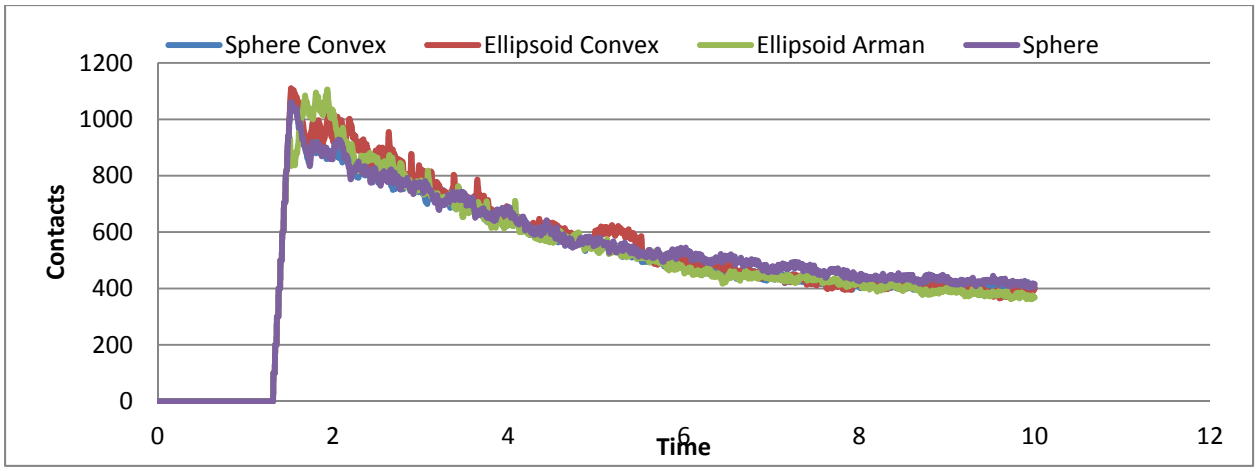

Figure 14: Contact Test 2, a 10x10x10 cube of spheres dropped onto a plate and allowed to flow off of it.

Conclusion

Simulating cohesion accurately is an important step in capturing rigid bod dynamics in a NEO (low gravity) environment. One of the largest factors that control the accuracy of the cohesion model is the stability of the LCP solver and the speed at which it converges to a solution. It is possible to control the convergence rate and interpenetration by stiffening the entire system. Unfortunately, this has the adverse effect of decreasing the stability of the LCP solver. It is possible to increase stiffness without decreasing the stability of the solver, by a combination of increasing the number of LCP iterations, increasing the LCP scaling factor and decreasing the timestep.

The short range force model has been added to the simulation capability and is currently being tested to make sure that the force models are being applied correctly. Once this is complete simulations of the anchor will be performed in a low gravity environment, where the effects that cohesion has on anchoring will be investigated. The goal of this effort is to simulate several different anchor designs, and at the end provide a recommendation on which type of anchor performs the best when tested against a range of parameters relating to soil, environment and anchor penetration angles/velocities.

Before the simulations of the anchor can be trusted, experimental validation needs to be completed. Macro level validation has been completed with the Brazil Nut and the Ball Drop simulations, where the behavior observed is similar to what was expected. When comparing actual simulation data to that presented in literature several problems are still being worked upon, with interpenetration playing a large role in the accuracy of a simulation. Validation and verification of the cohesion model and Chrono::Engine in general is currently being focused upon so that the anchoring tests can be performed with greater certainty.

Acknowledgements

The author would like to acknowledge the support of Marco Quadrelli, Abhi Jain, NASA JPL and in particular the DARTS Laboratory. The author would also like to thank the Simulation Based Engineering Laboratory, run by Prof. Dan Negrut, at the University of Wisconsin Madison for support on this project. This research was carried out at the Jet Propulsion Laboratory,

California Institute of Technology, and was sponsored by Space Grant and the National Aeronautics and Space Administration.

References

[1] A. Tasora, "Chrono::Engine Multibody Dynamics Engine," 2011. [Online]. Available: http://www.chronoengine.info/chronoengine/.

[2] NVIDIA Corporation, "Compute Unified Device Architecture (CUDA)," 2011. [Online]. Available: http://www.nvidia.com/object/cuda_home_new.html.

[3] Havok, "Havok Physics," 2011. [Online]. Available: http://www.havok.com/.

[4] NVIDIA Corporation, "PhysX," 2011. [Online]. Available: http://developer.nvidia.com/technologies/physx.

[5] J.-S. Pang and J. C. Trinkle, "Complementarity formulations and existence of solutions of dynamic multi-rigid-body contact problems with Coulomb friction," *Math. Program*, no. 73(2), pp. 199–226, 1996.

[6] M. Anitescu, F. A. Potra, and D. Stewart, "Time-stepping for three-dimensional rigid-body dynamics," *Computer Methods in Applied Mechanics and Engineering*, no. 177, pp. 183–197, 1999.

[7] R. W. Cottle and G. B. Dantzig, "Complementary pivot theory of mathematical programming," *Linear Algebra and Its Applications*, vol. 1, pp. 103–125, 1968.

[8] M. Anitescu and A. Tasora, "An iterative approach for cone complementarity problems for nonsmooth dynamics," *Computational Optimization and Applications*, 2008.

[9] D. J. Scheeres, C. M. Hartzell, P. Sanchez, and M. Swift, "Scaling forces to asteroid surfaces: The role of cohesion," p. 54, Feb. 2010.

[10] H. A. Perko, "Effects of surface cleanliness on lunar regolith mechanics.pdf," in *Proceedings of the Annual Meeting of the American Institute of Astronautics and Aeronautics*, 1996.

[11] A. Kudrolli, "Size separation in vibrated granular matter," *Reports on Progress in Physics*, vol. 67, no. 3, pp. 209-247, Mar. 2004.

[12] M. MacGregor, "Cracking the brazil nut effect," in *Colorado State Science Fair, Inc.*, 1996, pp. 1-20.

[13] D. I. Goldman, "Scaling and dynamics of sphere and disk impact into granular media," *Physical Review E*, vol. 77, no. 2, pp. 1-14, Feb. 2008.